

Technical Note

Objective evaluation method using multiple image analyses for panoramic radiography improvement

Satoshi IMAJO^{1,2,ABCF}, Yoshinori TANABE^{3,ABCDEF,*}, Nobue NAKAMURA^{2,BF}, Mitsugi HONDA^{2,CF}, Masahiro KURODA^{3,CF}

¹Department of Radiological Technology, Graduate School of Health Sciences, Okayama University, Japan

²Division of Radiology, Medical Support Department, Okayama University Hospital, Japan

³Department of Radiological Technology, Faculty of Health Sciences, Okayama University, Japan

*Corresponding author: Dr. Yoshinori Tanabe; tanabey@okayama-u.ac.jp

(received 16 December 2022; revised 20 January 2023; accepted 21 March 2023)

Abstract

Introduction: In the standardization of panoramic radiography quality, the education and training of beginners on panoramic radiographic imaging are important. We evaluated the relationship between positioning error factors and multiple image analysis results for reproducible panoramic radiography.

Material and methods: Using a panoramic radiography system and a dental phantom, reference images were acquired on the Frankfurt plane along the horizontal direction, midsagittal plane along the left–right direction, and for the canine on the forward–backward plane. Images with positioning errors were acquired with 1–5 mm shifts along the forward–backward direction and 2–10° rotations along the horizontal (chin tipped high/low) and vertical (left–right side tilt) directions on the Frankfurt plane. The cross-correlation coefficient and angle difference of the occlusion congruent plane profile between the reference and positioning error images, peak signal-to-noise ratio (PSNR), and deformation vector value by deformable image registration were compared and evaluated.

Results: The cross-correlation coefficients of the occlusal plane profiles showed the greatest change in the chin tipped high images and became negatively correlated from 6° image rotation ($r = -0.29$). The angle difference tended to shift substantially with increasing positioning error, with an angle difference of 8.9° for the 10° chin tipped low image. The PSNR was above 30 dB only for images with a 1-mm backward shift. The positioning error owing to the vertical rotation was the largest for the deformation vector value.

Conclusions: Multiple image analyses allow to determine factors contributing to positioning errors in panoramic radiography and may enable error correction. This study based on phantom imaging can support the education of beginners regarding panoramic radiography.

Keywords: panoramic radiography; quantitative evaluation; deformable image registration; peak signal-to-noise ratio.

Introduction

Panoramic radiography provides a comprehensive view of dentition and is widely used for diagnosis and orthodontics in the oral cavity.¹ Panoramic radiography uses thin X-rays with a slit to synchronize the rotational orbit of the X-ray tube and detector, resulting in blurred imaging except for the target area of a certain thickness.¹ As jaw dentition varies from patient to patient and the instrument has a limited rotational orbit and tomographic range, the slightest positioning error reduces image quality and may compromise the diagnostic accuracy.²

Previous research on positioning errors and quality assessment of panoramic radiographic images has determined that approximately 11% of clinical images are error-free, while most

images have some kind of positioning error.³ The positioning of panoramic radiographs should be vertical on the midsagittal plane and horizontal on the Frankfurt plane⁴, however, no specific indicator is given for the angle on the occlusal plane, which is considered ideal in the imaging results. This ambiguity is one of the reasons for positioning errors and low reproducibility. The lack of objective criteria for evaluating imaging results can easily lead to subjectivity in educational guidance for panoramic radiography, thus hindering positioning training.

In radio diagnostic and radiotherapy images, various image quality evaluations and image analysis methods using phantom are effective for image quality improvement and quality control.⁵⁻⁷ The peak signal-to-noise ratio (PSNR) and

deformable image registration (DIR) have been used as objective evaluation methods for radiographic imaging and radiotherapy positioning.⁸⁻¹⁰ These evaluation methods often use a single analysis method to evaluate positioning errors. We consider that positioning errors in panoramic radiographs may be qualitatively evaluated by using multiple image analyses, and positioning errors can be used to educate beginners based on objective quantities. To the best of our knowledge, no previous studies exist on the evaluation of positioning errors in panoramic radiographs based on multiple analyses. Thus, we objectively evaluated the characteristics of positioning errors according to the cross-correlation coefficient, angle, PSNR, and DIR of the occlusal plane profile of panoramic radiographs using images acquired from a skull phantom. This study may support the education of beginners on panoramic radiographic imaging and training in radiographic imaging as well as standardization of panoramic radiography quality.

Methods

Equipment and reference imaging

The equipment used was a panoramic radiography system model Veraview epocs X550 (MORITA, Kyoto, Japan) and an SK100 skull phantom (The Phantom Laboratory, Salem, NY) to capture images of the reference positioning with the midsagittal plane vertical, Frankfurt plane horizontal, and canine teeth centered in the tomographic region in the forward-backward direction.

Image analysis was performed using ImageJ/Fiji version 1.53f51 (National Institutes of Health, Bethesda, MD, USA) to analyze occlusal plane profile plots, PSNR, and DIR. Statistical analysis was performed using JMP Pro 15.0 statistical software (SAS, Cary, NC, USA). The flowchart of this study is shown in **Figure 1**. Cross-correlation analysis was used to evaluate the change of occlusal plane profiles for positioning error¹¹, and PSNR was used to evaluate the displacement of the thin fault zone by positioning error^{10,12}. DIR was used to evaluate the displacement of the structure by positioning errors¹³.

Positioning error in phantom imaging

A skull phantom was imaged with three types of positioning errors with respect to the reference positioning (**Figure 1a**). First, images with positioning errors were captured by translating the skull phantom by 1, 2, 3, 4, and 5 mm toward the front or back relative to the tomographic center at the canine tooth. Next, images with positioning errors of rotation were captured with the chin tipped high and down rotated by 2, 4, 6, 8, and 10° with respect to the midsagittal plane, and right and left side tilted images were captured with horizontal rotations of 2, 4, 6, 8, and 10° with respect to the Frankfurt plane. For rotation of the midsagittal plane, all analysis results were evaluated by averaging the left and right side tilted results of image analysis owing to the imperfect left-right asymmetry structure of the skull phantom.

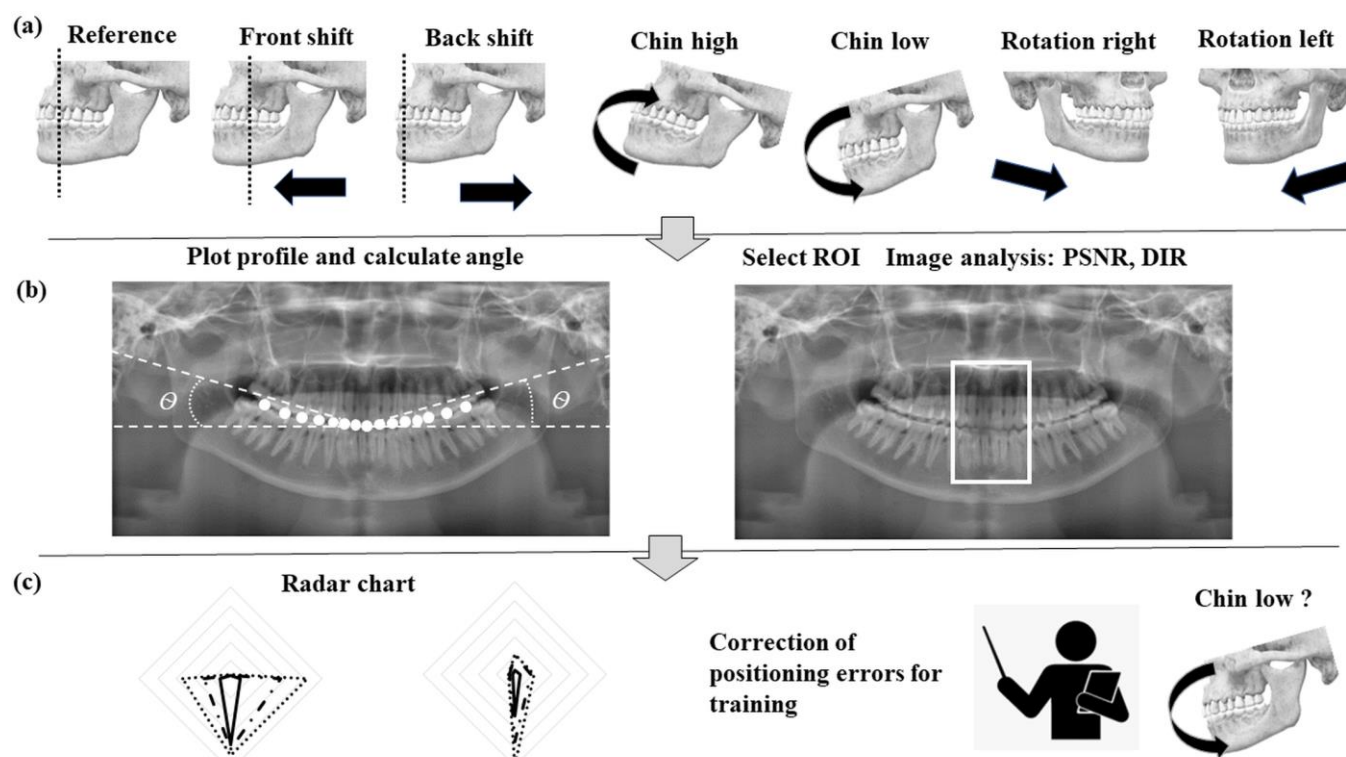


Figure 1. Flow of the present study, (a) taking reference images and positioning errors, (b) image analysis of panoramic radiographic images; calculation of occlusal plane profile and occlusal angle, calculation of PSNR and deformation vector value for the region of interest, and (c) education using image analysis and radar chart analysis of positioning errors.

Cross-correlation analysis of occlusal plane profiles

The occlusal plane profile of a panoramic radiograph was manually plotted the profile three times repeatedly by the radiologist using ImageJ/Fiji and averaged the results (**Figure 1b**). The plotted coordinates were entered into Excel (Microsoft, Redmont, WA, USA), and the cross-correlation coefficient was calculated for the cephalocaudal shift of the occlusal plane profile relative to the distance (x) of the profile as follows¹⁴:

$$\text{Cross correlation coefficient } (X, Y) = \frac{\sum(x-\bar{x})\sum(y-\bar{y})}{\sqrt{\sum(x-\bar{x})^2\sum(y-\bar{y})^2}} \quad \text{Eq. 1}$$

The left–right angle of each image was then calculated by averaging the difference between the angle from the center to the third molar in the curve of the occlusal plane and left–right angle from the reference image.

Evaluation of positioning error based on PSNR

A region of interest (ROI) was selected on the panoramic radiograph reference and positioning error images centered on the mid-sagittal plane at 5.30×6.25 cm (area of left and right lateral incisors in the reference image), as shown in **Figure 1b**. To evaluate image quality deterioration and blurring for the displacement of the thin fault zone due to positioning errors, the PSNR (in decibels (dB)) was calculated for the ROI between the panoramic radiograph reference and positioning error images using ImageJ/Fiji as follows¹⁰:

$$\text{PSNR} = 10 \times \log_{10} \frac{\text{MAX}^2}{\text{MSE}} \quad \text{Eq. 2}$$

where MAX is the maximum pixel intensity in the ROI and MSE is the mean squared error between the reference and positioning error images.

Evaluation of positioning errors based on deformation vector value by deformable image registration

To evaluate the displacement of structures from the reference image due to positioning errors, the deformable image registration (DIR) was performed between the panoramic radiograph reference and positioning error images using the bUnwarpl function of ImageJ/Fiji with the ROIs described in Sect. 2.4.⁹ For registration, an approximation based on the B-spline function was used to calculate the distance between the features as a deformation vector value (optimal direct similarity error) using the corresponding signal value between the reference and positioning error images as the feature value. The deformation vector value of the initial registered image and mid-treatment registered image was determined using the following equation^{15,16}:

$$\text{Deformation vector value} = \frac{1}{\#\Omega} \sum_{x \in \Omega} [I_d(x) - I_i(g(x))]^2 \quad \text{Eq. 3}$$

Where $g(x)$ is to find a function for the goal of image registration: it maps coordinates from the positioning error images image intensity (I_d) onto the reference image intensity (I_i), so that $I_i(g(x))$ (a deformed version of the reference image) resembles $I_d(x)$ as much as possible.^{16,17}

Radar chart and statistical analysis of positioning error image analysis

The cross-correlation coefficients of the occlusal plane profiles and deformation vector value owing to the left-right angle difference, PSNR, and DIR were normalized to 1, according to the maximally degraded value and plotted in a radar chart. The results per image evaluation were subjected to multivariate correlation analysis. Correlation coefficients (r) were determined by linear approximation using JMP Pro 15.0 (SAS Institute Inc., Cary, NC, USA).

Results

Table 1 lists the cross-correlation coefficients of the occlusal plane profiles from the reference and positioning error images and the left-right angle difference, PSNR, and deformation vector value by DIR. In all the image analyses, the translation shift in the forward–backward direction did not change substantially compared with the positioning error in the rotational direction. However, the angle difference from the reference image changed from 0.2° at 1-mm translation in the backward direction to 2° at 5-mm translation, and the angle difference tended to increase with the positioning error.

Figure 2 shows the results of the representative occlusal plane profiles. The cross-correlation coefficient of the occlusal plane profile had a negative correlation ($r = -0.29$) with positioning errors in the chin tipped high direction at an angle of 6° or higher, and the highest negative correlation ($r = -0.66$) occurred at 10° (**Table 1, Figure 2**). In the analysis of positioning errors in the vertical rotation of the midsagittal plane, the PSNR (13.5 dB) and deformation vector value (892.5) were the lowest at a rotation angle of 10° , resulting in the image with the lowest image similarity among those with positioning errors (**Table 1**).

The radar charts of the evaluation results are shown in **Figure 3**, where the largest positioning error defines the normalization to 1. The positioning error along the translational direction in the front–back direction resulted in the smallest error change (**Figure 3**). The positioning error in the vertical rotation direction showed a characteristic radar chart with large PSNR and deformation vector value, and the horizontal displacement showed a characteristic radar chart with large changes in the cross-correlation coefficient and left–right angle difference (**Figure 3**).

Table 1. Evaluation of image quality for panoramic radiographs.

	Positioning error (Shift or rotation)	Cross-correlation coefficient	Average difference angle between right and left (°)	Average PSNR (dB)	Average vector displacement
Forward shift	1 mm	0.99	0.56	26.30	22.65
	2 mm	0.96	1.40	24.44	30.02
	3 mm	0.96	1.86	23.55	50.70
	4 mm	0.86	1.92	23.43	57.75
	5 mm	0.90	2.18	23.13	62.03
Backward shift	1 mm	0.99	0.18	30.39	23.80
	2 mm	0.97	0.88	28.27	23.35
	3 mm	0.95	1.47	25.55	33.54
	4 mm	0.86	1.43	24.12	45.77
	5 mm	0.89	2.14	23.49	54.30
Chin high	2°	0.86	2.43	22.98	112.46
	4°	0.59	3.68	19.74	160.57
	6°	-0.28	5.94	19.58	266.24
	8°	-0.44	6.57	19.34	445.36
	10°	-0.66	10.68	16.40	469.98
Chin low	2°	0.93	1.03	18.24	194.15
	4°	0.91	3.64	17.98	256.94
	6°	0.92	5.75	17.55	378.18
	8°	0.88	7.05	16.78	486.92
	10°	0.90	8.87	16.35	538.89
Tilt to side	2°	0.93	0.42	22.67	110.62
	4°	0.80	1.17	19.85	170.52
	6°	0.66	1.47	18.06	229.54
	8°	0.72	1.72	15.17	367.81
	10°	0.65	2.50	13.53	892.54

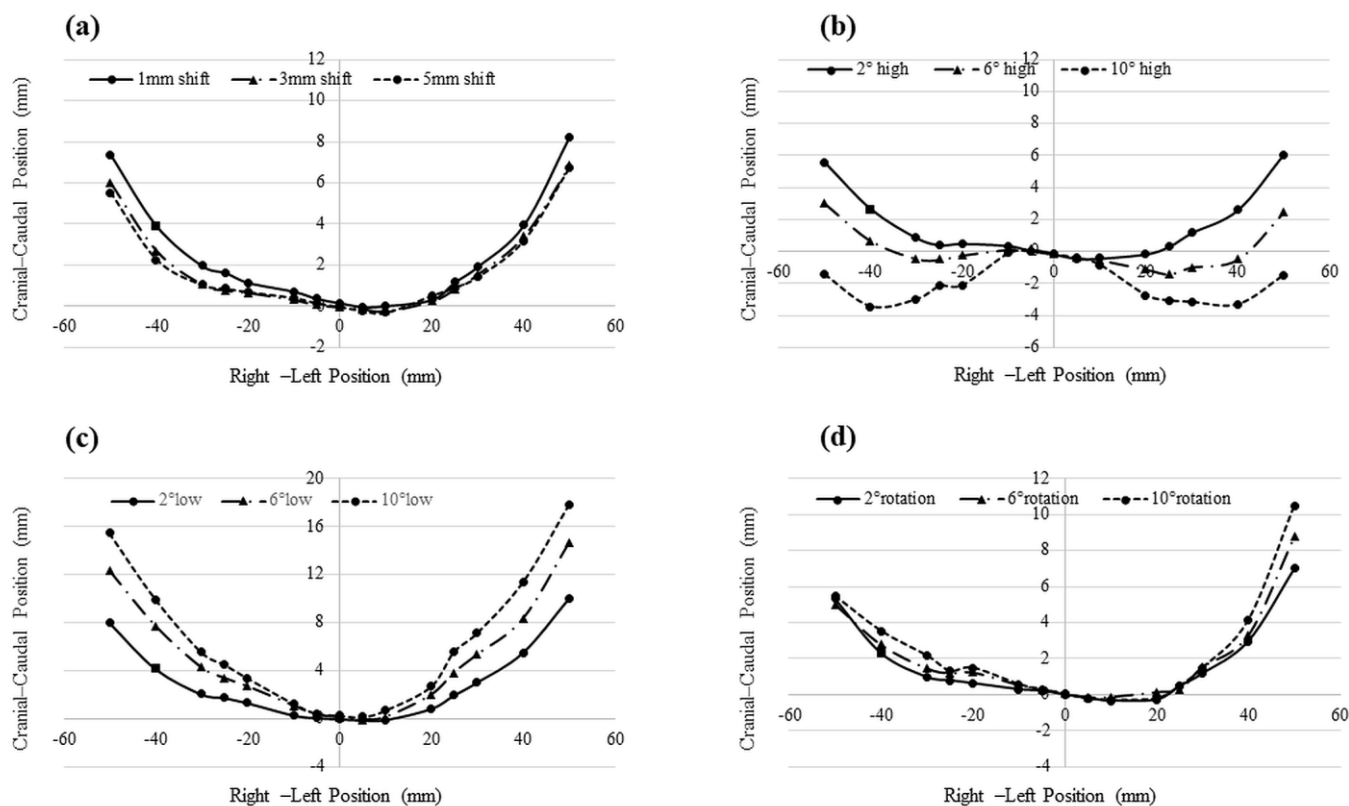


Figure 2. Occlusal plane profiles of characteristic positioning errors; (a) forward shift, (b) chin tipped high, (c) chin tipped low, and (d) rightward.

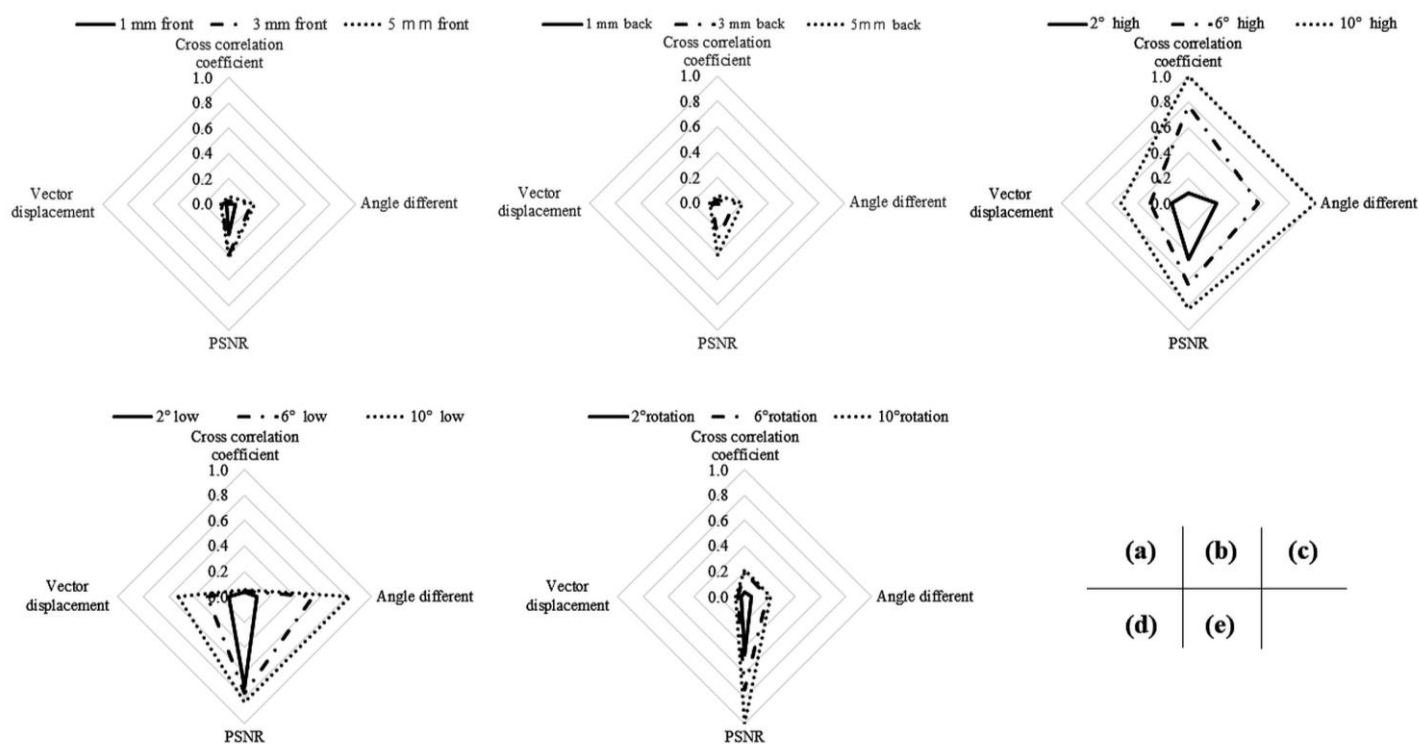


Figure 3. Radar chart of characteristic positioning errors; (a) forward shift, (b) backward shift, (c) chin tipped high, (c) chin tipped low, and (d) average of right and left side tilted.

Table 2. Relationship of correlation coefficient for image analysis.

r	Cross-correlation coefficient	Average difference angle for reference image	PSNR	Average deformation vector value
Cross-correlation coefficient	-	-0.65	0.38	-0.42
Average difference angle for reference image	-0.65	-	-0.58	0.62
PSNR	0.38	-0.58	-	-0.85
Average deformation vector value	-0.42	0.62	-0.85	-

Table 2 lists the results of multivariate correlation analysis for the image evaluations. The highest correlation coefficients were PSNR and deformation vector value ($r = 0.85$), while the cross-correlation coefficients of the occlusal plane profile, deformation vector value, and left–right angle difference were weakly correlated ($r = 0.38$). All the left–right angle differences showed a moderate or better correlation ($r > 0.58$).

Discussion

In the present study, positioning errors were evaluated using the cross-correlation coefficient between panoramic radiograph reference and positioning error images regarding the occlusal plane profile and its left–right angle difference, PSNR, and deformation vector value.

The cross-correlation coefficients of the occlusal plane profiles decreased for all the indicators with increasing positioning error. The occlusal plane is based on a gentle angle in panoramic radiography, but with the chin tipped high, the angle becomes parallel and the jaw area is enlarged, while with the chin tipped low, the tip of the jaw becomes elongated and V-shaped.¹⁸ The phase of the occlusal plane profile allows for the easy detection of errors in the correlation coefficient of the occlusal plane profiles. The anterior teeth and lateral incisors are blurred in with the chin tipped high/low, likely because they are displaced from the thin fault zone of the anterior teeth.^{18,19} In addition, the PSNR and deformation vector value have low similarities. The angle of the occlusal plane profile tends to vary among radiographers and patients⁸, and establishing a specific angle to obtain a gentle curve of the occlusal plane profile can lead to high reproducibility in imaging and improve the education of beginners.

With regard to the angle difference of the occlusal plane profile with respect to the reference image, the deviation tended to increase with the positioning error. This is possibly because the panoramic X-ray tube rotates around the subject in multiple axes in the mechanism, and the magnification and reduction rates differ depending on the positioning of the X-ray tube and the patient. In addition, the rotation may be identified by evaluating the angle difference between the left and right angles and the magnification rate in addition to the angle difference from the reference image. This is because the vertical rotation trajectory and misalignment of the patient's positioning produce asymmetry between the left and right regions.²⁰ Regarding the difference from the reference angle, the cross-correlation coefficient of the occlusal plane profile, PSNR, and deformation vector value showed moderate correlations, suggesting that it can be used as a simple evaluation indicator.

The PSNR decreases in image similarity as the positioning error increases, possibly owing to the blur on the image that shifts from the fault zone and the asymmetry of the subject as major factors. In general, the PSNR should be at least 30 dB to indicate no deterioration in image quality.²¹ In this study, only a 1-mm shift in the backward direction provided a PSNR above 30 dB (i.e., 30.4 dB).¹⁰ As the PSNR allows to easily evaluate positioning errors under shifts of a few millimeters, it can be used as an objective indicator for radiography education.

The deformation vector value for DIR is the largest for a horizontal rotation, possibly owing to the large change in the displacement of the anterior tooth density. Thus, this displacement allows clinicians to evaluate whether the position is centered on the midsagittal plane. In addition, the PSNR quantifies the displacement, whose direction can be obtained as a deformation vector value from DIR⁹, facilitating objective image-based guidance.

The radar chart illustrates the differences in the forward–backward and rotational directions for positioning errors. The forward–backward direction shows less change compared with rotations. The positioning error of horizontal rotation shows that the cross-correlation coefficient of the occlusal plane profile is larger with the chin tipped high than for a vertical rotation, and the angle difference from the reference image is larger with the chin tipped low. In addition, the deformation vector value changes substantially for a vertical rotation, suggesting a large shift in the midsagittal plane of the image. The radar chart trends may allow to intuitively correct positioning errors and evaluate beginner education and imaging training. In addition, obtaining the area and average score of the radar chart of multiple image

analyses can be used as a numerical index for the training results of educating beginners before clinical practice. One of the causes of positioning errors in the panoramic radiograph is the ambiguity of the criteria positioning errors. The evaluation index and method of this study will improve technology and the reproducibility of clinical panoramic X-ray images through education. In recent years, several technologies and education methods using video and manual text have been studied to support the positioning of panoramic radiograph^{1,22}. The combination of education and development tools will help provide higher-quality images.

Limitations

A limitation of this study is that the positioning error cannot be directly evaluated in clinical practice without reference images. However, we believe that the reproducibility of imaging can be improved by determining the cross-correlation coefficients of occlusal plane profiles as well as by criteria and tolerance levels of angle differences at different institutions. Another limitation of this study is the limited image analysis and the use of a single skull phantom. In this study, we indicated significant changes in the positioning error of the panoramic X-ray for the translation shift and the rotation using some image analysis. However, the phantoms of the facilities are different, so we consider that each facility must investigate objective numerical values before educational guidance. In addition, a panoramic radiograph becomes blurred when it deviates from the tomographic region. Therefore, a more accurate evaluation can be achieved by using frequency analysis or a modulation transfer function to analyze the blur in low frequencies.^{23,24}

Conclusion

We evaluated the positioning errors considering cross-correlation coefficients of the occlusal plane profile and the deformation vector value in terms of the left–right angle difference, PSNR, and DIR for panoramic radiographs. The results from multiple image analyses showed specific trends for horizontal and vertical displacements, providing objective indicators for correcting positioning errors. This study may contribute to the education and training of beginners in panoramic radiography by using phantoms and to the design of imaging systems.

References

1. Różyło-Kalinowska I. Panoramic radiography in dentistry. *Clin Dent Rev*. 2021;5(26):1-10. <https://doi.org/10.1007/s41894-021-00111-4>
2. Martins LAC, Nascimento EHL, Gaêta-Araujo H, et al. Mapping of a multilayer panoramic radiography device. *Dentomaxillofac Radiol*. 2022;51(4):20210082. <https://doi.org/10.1259/dmfr.20210082>
3. Dhillon M, Raju SM, Verma S, et al. Positioning errors and quality assessment in panoramic radiography. *Imaging Sci Dent*. 2012;42(4):207-12. <https://doi.org/10.5624/isd.2012.42.4.207>
4. Mckee I W, Glover KE, Williamson PC, et al. The effect of vertical and horizontal head positioning in panoramic radiography on mesiodistal tooth. *Angle Orthod*. 2001;71(6):442-51. [https://doi.org/10.1043/0003-3219\(2001\)071<0442:TEOVAH>2.0.CO;2](https://doi.org/10.1043/0003-3219(2001)071<0442:TEOVAH>2.0.CO;2)
5. Manson EN, Mumuni AN, Shirazu I, et al. Development of a standard phantom for diffusion-weighted magnetic resonance imaging quality control studies: A review. *Polish J Med Phys Eng*. 2022;28(4):169-179. <https://doi.org/10.2478/pjmpe-2022-0020>
6. Bąk B, Skrobała A, Adamska A, et al. Evaluation and risk factors of volume and dose differences of selected structures in patients with head and neck cancer treated on Helical TomoTherapy by using Deformable Image Registration tool. *Polish J Med Phys Eng*. 2022;28(2):60-68. <https://doi.org/10.2478/pjmpe-2022-0007>
7. Ximenes AD, Anam C, Hidayanto E, et al. Automation of slice thickness measurements in computed tomography images of AAPM CT performance phantom using a non-rotational method. *Polish J Med Phys Eng*. 2022;28(3):133-138. <https://doi.org/10.2478/pjmpe-2022-0016>
8. Tanabe Y, Ishida T. Automated Detection of Respiratory Movements for Image Quality Assurance. *J Med Imaging Health Inf*. 2020;10(7):1473-8. <https://doi.org/10.1166/jmihi.2020.3039>
9. Tanabe Y, Ishida T. Development of a novel detection method for changes in lung conditions during radiotherapy using a temporal subtraction technique. *Phys Engin Sci Med*. 2021;44(2):1341-50. <https://doi.org/10.1007/s13246-021-01070-7>
10. Tanabe Y, Ishida T. Quantification of the accuracy limits of image registration using peak signal-to-noise ratio. *Radiol Phys Technol*. 2017;10(1):91-4. <https://doi.org/10.1007/s12194-016-0372-3>
11. Tanabe Y, Kiritani M, Deguchi T, et al. Patient-specific respiratory motion management using lung tumors vs fiducial markers for real-time tumor-tracking stereotactic body radiotherapy. *Phys Imaging Radiat Oncol*. 2022;25:100405. <https://doi.org/10.1016/j.phro.2022.12.002>
12. Agarwal S, Agarwal A, Deshmukh M. Denoising images with varying noises using autoencoders. In: Nain N, Vipparthi S, Raman B. (eds) *Computer Vision and Image Processing. CVIP 2019. Communications in Computer and Information Science*. 2020;1148:3-14. https://doi.org/10.1007/978-981-15-4018-9_1
13. Tanabe Y, Ishida T, Eto H, et al. Evaluation of the correlation between prostatic displacement and rectal deformation using the Dice similarity coefficient of the rectum. *Med Dosim*. 2019;44(4):e39-e43. <https://doi.org/10.1016/j.meddos.2018.12.005>
14. Tanabe Y, Tanaka, H. Statistical evaluation of the effectiveness of dual amplitude-gated stereotactic body radiotherapy using fiducial markers and lung volume. *Phys Imaging Radiat Oncol*. 2022;24:82-87. <https://doi.org/10.1016/j.phro.2022.10.001>
15. Oh S, Kim S. Deformable image registration in radiation therapy. *Rad Oncol J*. 2017;35:101-11. <https://doi.org/10.3857/roj.2017.00325>
16. Arganda-Carreras I, Sorzano COS, Kybic J, Ortiz-de-Solorzano C. bUnwarpJ: Consistent and elastic registration in ImageJ. *Methods and applications. Second ImageJ User & Developer Conference*. 2008
17. Sorzano CO, Thévenaz P, Unser Ms. Elastic registration of biological images using vector-spline regularization. *IEEE Trans Bio Med Eng*. 2005;52(4):652-63. <https://doi.org/10.1109/TBME.2005.844030>
18. Kattimani S, Kempwade P, Ramesh DNSV, et al. Determination of different positioning errors in digital panoramic radiography: a retrospective study. *J Med Radiol Pathol Surg*. 2019;6(2):5-8. <https://doi.org/10.15713/ins.jmrps.159>
19. Pawar R, Makdissi J. The role of focal block (trough/plane) in panoramic radiography: why do some structures appear blurred out on these images? *Radiography*. 2014;20(2):167-70. <https://doi.org/10.1016/j.radi.2013.11.004>
20. Rondon RHN, Pereira YCL, Nascimento GC. Common positioning errors in panoramic radiography: a review. *Imaging Sci Dent*. 2014;44(1):1-6. <https://doi.org/10.5624/isd.2014.44.1.1>
21. Setiadi DRIM. PSNR vs SSIM: imperceptibility quality assessment for image steganography. *Multimedia Tools and Applications*. 2021;80(6):8423-44. <https://doi.org/10.1007/s11042-020-10035-z>
22. Grillon M, Yeung AWK. Content Analysis of YouTube Videos That Demonstrate Panoramic Radiography. *Healthcare*. 2022;10(6):1093. <https://doi.org/10.3390/healthcare10061093>
23. Tanabe Y, Ishida T. Development of a quantitative method based on the hill-shading technique for assessing morphological changes in the bone during Image-Guided Radiotherapy for Bone Metastasis. *J Med Imaging Health Inf*. 2021;11(8):2173-7. <https://doi.org/10.1166/jmihi.2021.3818>
24. Hernandez AM, Wu PM, Siewerdsen JH, et al. Location and direction dependence in the 3D MTF for a high-resolution CT system. *Med Phys*. 2021;48(6):2760-71. <https://doi.org/10.1002/mp.14789>